AN ACCELERATED SURFACE-HOPPING METHOD FOR COMPUTATIONAL SEMICLASSICAL MOLECULAR DYNAMICS

by

Laren K. Mortensen

A senior thesis submitted to the faculty of

Brigham Young University

in partial fulfillment of the requirements for the degree of

Bachelor of Science

Department of Physics and Astronomy

Brigham Young University

April 2007

BRIGHAM YOUNG UNIVERSITY

DEPARTMENT APPROVAL

of a senior thesis submitted by

Laren K. Mortensen

This thesis has been reviewed by the research advisor, research coordinator, and department chair and has been found to be satisfactory.

Date	Bret C. Hess, Advisor
Date	Eric Hintz, Research Coordinator
Date	Scott D. Sommerfeldt, Chair

ABSTRACT

AN ACCELERATED SURFACE-HOPPING METHOD FOR COMPUTATIONAL SEMICLASSICAL MOLECULAR DYNAMICS

Laren K. Mortensen

Department of Physics and Astronomy

Bachelor of Science

We improved on the surface-hopping method of John C. Tully (1990) by eliminating the rapidly oscillating phase factors from the method. This allows for a significantly larger time step in the surface-hopping method. We also used a second-order taylor series approximation instead of a constant Hamiltonian for the time steps.. We used time-dependent perturbation theory to symbolically solve for the propagation of the wavefunction. We compare the two methods using a simple four-state one-dimensional model. Accuracy was determined by comparing switching probabilities and expansion coefficients for different time step sizes. Our comparisons show the accelerated method runs five to ten times faster for the same level of accuracy.

Contents

Table of Contents **5**

1 Introduction **1**
1.1 Motivations for Semiclassical Molecular Dynamics 1
1.2 Tully's Surface Hopping Method 3
1.3 Advantages and Limitations of Tully's Surface-Hopping Method . . . 7

2 The Method **8**
2.1 Motivation for Accelerated Method 8
2.2 Interaction Picture Representation 10
2.3 2nd Order Hamiltonian Approximation 11
2.4 First Order Symbolic Solution 12

3 Results and Conclusions **15**
3.1 Test Model 15
3.2 Method of Comparison and Results 16
3.3 Results and Conclusions. 20

Bibliography **23**

Chapter 1

Introduction

1.1 Motivations for Semiclassical Molecular Dynamics

In photophysics, there is an increasing need to be able to simulate molecular interactions with excited state molecules. One process being studied is titanium-dioxide photocatalysis. One exciting possibility for this catalyst is the splitting of water into hydrogen and oxygen gas using sunlight. This creates the possibility of using sunlight to obtain hydrogen gas for fuel cells.

Photo-excited electron transitions are important for the effect and are being studied. These interactions are difficult to study with quantum mechanics fully, due to the difficulty of simulating many nuclei and electrons. Semiclassical molecular dynamics uses the approach of simulating the nuclei classically, and the electrons quantum mechanically. This approach offers the advantages of incorporating electronic quantum effects, but with much less computational intensity than a full quantum mechanical treatment.

The use of classical physics for nuclear motion is the Born-Oppenheimer approx-

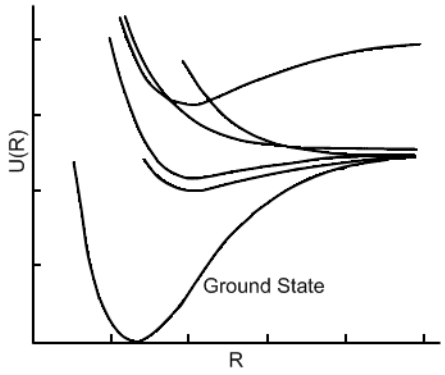

Figure 1.1 Adiabatic potential energy curves vs bond distance R of a typical diatomic molecule [1]. The excited adiabatic energy states are close enough to have significant nonadiabatic coupling. The ground state does not have significant coupling unless the molecule has enough kinetic energy.

imation. The Born-Oppenheimer approach is an adiabatic approximation where the nuclear motion is slow enough that the much faster electrons see a slowly changing potential. This works well for low kinetic energies because the nuclear masses are much greater than the electrons' masses. However, at high kinetic energy the nuclear motion is fast enough to trigger state transitions. The system can no longer be treated adiabatically. Figure 1.1 shows the typical potential energy vs. bond distance curves of a diatomic molecule. The excited states energies are close enough that electronic state coupling cannot be ignored [1].

Tully' derives a semiclassical molecular dynamics method that models nonadiabatic transitions. In this paper we attempt to improve on the work of John C. Tully by accelerating his computational method [2]. The remainder of the introduction is a brief overview of Tully's surface-hopping method. In chapter two, we solve for an accelerated method that reduces the computations and maintains the same level of accuracy. In chapter three, we compare our accelerated method using computation times and accuracy with a simple one-dimensional four-state model.

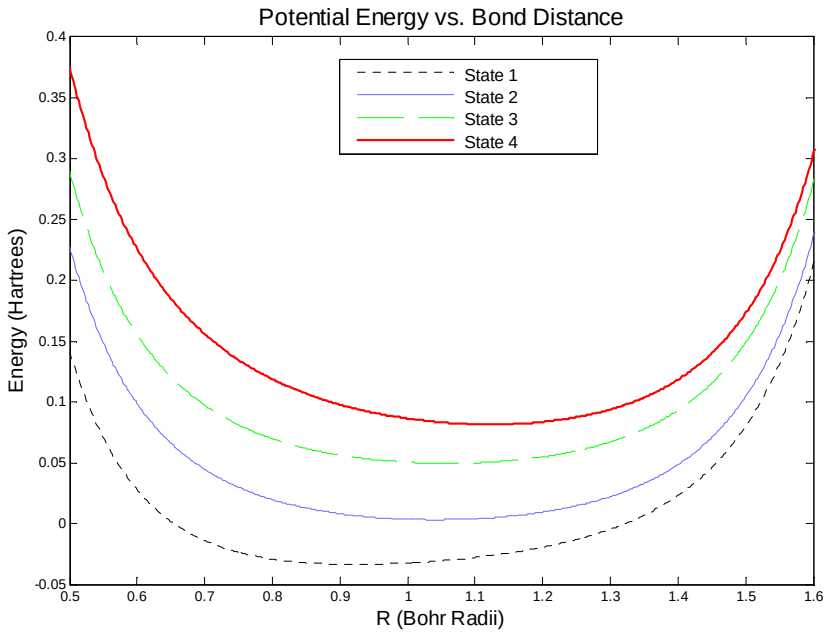

Figure 1.2 Hypothetical potential energy adiabatic curves of a simple four state model. The surface hopping method models transitions as instant jumps between the adiabatic surfaces. In this example a nucleus is in ground state and is excited to state 4 and falls back down to state 3.

1.2 Tully's Surface Hopping Method

Semiclassical molecular dynamics uses the Born-Oppenheimer adiabatic approximation in which nuclear motion is treated classically using adiabatic electronic state potentials. The nuclear motion can be treated classically because the nuclear masses are very large. Each electronic state is a potential energy surface that governs the nuclear motion.

One of the important assumptions of semiclassical molecular dynamics is that the nuclear forces change adiabatically. The surface hopping method has the purpose of modeling nonadiabatic transitions so that the molecular dynamic approach can still be used. The surface-hopping method models transitions as an instant jump between two Born-Oppenheimer adiabatic surfaces. The nuclei then follow a new trajectory along the new adiabatic potential energy surface with an adjusted kinetic energy to

conserve energy. An example is shown in Fig. 1.2. The figure shows a hypothetical four state model. In the figure a nucleus starts in the ground state and is excited to the fourth state and later drops back down to the third state.

Tully points out that a switch between two potentials must be made at some point because a particle can't remain in a superposition of states indefinitely. The particle must be in one state or the other after it has left the area of strong coupling. For example, a particle might be trapped in one state, and unbound in another. The particle can't be correctly modeled by a superposition of those two states.

Tully's surface-hopping method has the advantage of allowing transitions to occur anywhere along the potential energy surface not just at localized avoided crossings where the coupling is strongest. Tully's approach also has the advantage of allowing any number of different coupled states. The rest of this section is an overview of Tully's surface-hopping method [2].

Tully derives that the strength of the interaction energy between states is dependent on the strength of the coupling and the velocity of the nuclei.

$$\tilde{\mathbf{H}} = -i\hbar\dot{\mathbf{R}} \cdot \mathbf{d_{kl}} \tag{1.1}$$

In this expression $\mathbf{R}$ designate nuclear positions. The dot product represents a time derivative of $\mathbf{R}$, or the nuclear velocities. The strength of the coupling is defined by $\mathbf{d}_{kj}$ which Tully calls the "nonadiabatic coupling vector."

$$\mathbf{d}_{ij}(\mathbf{R}) = \langle \phi_i(\mathbf{r}, \mathbf{R}) | \nabla_{\mathbf{R}} \phi_j(\mathbf{r}, \mathbf{R}) \rangle. \tag{1.2}$$

The functions $\phi_j(\mathbf{r}, \mathbf{R})$ are a set of orthonormal electronic basis functions that are eigenstates of the adiabatic potentials.The brackets represent integration over electronic coordinates only. We can represent the wave function $\Psi(\mathbf{r}, \mathbf{R}, \mathbf{t})$ for the system

as a combination of these orthonormal basis states,

$$\Psi(\mathbf{r}, \mathbf{R}, t) = \sum_j c_j(t)\ \phi_j(\mathbf{r}, \mathbf{R}) \tag{1.3}$$

where $c_j(t)$ are the complex valued expansion coefficients. Using Eqs. (1.3), (1.1) Schrodinger's equation,

$$\begin{aligned} i\hbar\frac{\partial\,\mathbf{\Psi}}{\partial t} &= \mathbf{H}\,\mathbf{\Psi} \\ &= (\mathbf{H_0} + \tilde{\mathbf{H}})\mathbf{\Psi} \end{aligned} \tag{1.4}$$

becomes

$$i\hbar\dot{c}_k = E_{0k}\,c_k + \sum_j -i\hbar\ c_j\ \mathbf{R}\cdot\mathbf{d_{kj}} \tag{1.5}$$

where E_{0k} are the diagonal elements of $\mathbf{H_0}$.

In his paper, Tully uses density matrix notation because it is more general.

$$a_{kj} = c_k c_j^* \tag{1.6}$$

In density matrix notation Eq. (1.5) becomes

$$i\hbar\dot{a}_{kj} = \sum_l -i\hbar\ a_{lj}\ \mathbf{R}\cdot\mathbf{d_{kl}} + i\hbar\ a_{kl}\mathbf{R}\cdot\mathbf{d_{lj}}. \tag{1.7}$$

The diagonal matrix elements a_{jj} are electronic state populations and the off-diagonal matrix elements define the coherence. Tully defines a four step algorithm for modeling nonadiabatic transitions, paraphrased below.

Step 1. Input initial conditions. This includes all nuclear positions and momenta. Also electronic state densities need to be initialized. Typically, the simulation will begin in one initial state, however this need not be the case.

Step2. The motion of the nuclei are calculated for a small time step Δt along the potential energy surface of the current state. Tully uses the Runga-Kutta-Gill [3] method as do we because the method only needs the current position of the particle

and the potentials. After the nuclear motion is propagated, the density of states matrix is integrated along the nuclear trajectory using Eq. (1.7). The time step Δt must be small enough for the electronic density elements to not change significantly.

Step 3. The switching probabilities from the current state to all other states are then calculated. The diagonal density elements a_{jj} are the electronic state populations. The diagonal matrix elements have a time derivative

$$\dot{a}_{kk} = \sum_{l \neq k} b_{kl},$$

where

$$b_{kl} = 2\hbar^{-1} Im(a^*_{kl} V_{kl}) - 2Re(a^*_{kl} R \cdot d_{kl}). \tag{1.8}$$

Tully proposes using a least switches algorithm to minimize the number of switches, but still maintain the correct populations. The switching probabilities, g_{kj}, from state k to state j are

$$g_{kj} = \frac{\Delta t b_{jk}}{a_{kk}}.$$

If the switching probability g_{kj} is negative it is set to zero. A uniform random number, $0 < \zeta < 1$, is selected to determine if a switch to state j is invoked. For example if $k = 1$, a switch to state 2 is invoked if $\zeta > g_{12}$. A switch to state 3 is invoked if $g_{12} < \zeta < g_{12} + g_{13}$, etc.

Step 4. If no switch is invoked, return to step 2. If a switch is invoked, the particle will now trace a trajectory on the new potential for its new electronic state. The velocity of the particle is adjusted in the direction of the nonadiabatic coupling vector d_{kk}. If the particle has insufficient kinetic energy to jump to the higher potential energy surface, the jump is not allowed. Return to step 2.

This process is repeated until the simulation is completed. To obtain significant statistical results, the simulation must be repeated several times for each set of initial conditions of interest.

1.3 Advantages and Limitations of Tully's Surface-Hopping Method

The main advantage to Tully's Surface Hopping Method is its practicality while correctly modeling many quantum mechanical effects. The method models nonadiabatic effects simply with much less computational intensity than a full quantum mechanics treatment. The method has the advantage of allowing any number of different coupled electronic states and allows transitions to occur at any point on the potential. It allows simulations in full dimensionality easily because of the use of classical molecular dynamics.

However, much of this practicality comes at a cost of neglecting several quantum effects. The model takes no account of tunneling, zero-point motion, level quantization, or nuclear quantum effects. The model also has the approximation of nuclear motion being restricted to a single potential with instant jumps during transitions.

Tully's method is best suited for simulations with high kinetic energies and significant electronic coupling. With high kinetic energy, many of the ignored quantum effects are negligible. The most computational intensive calculations are the changes in the electronic state expansion coefficients, $c_j(t)$. The electronic state populations require much smaller time steps than the nuclear motion due to the rapidly changing phases of the high-energy states.

We propose a method to reduce the computational intensity of this part of the algorithm. We solve symbolically for a second order approximation of the time derivative of the density of states. With this approximation we can integrate over the time scale of the nuclear motion instead of the time scale of the electronic phase information.

Chapter 2

The Method

2.1 Motivation for Accelerated Method

We start with the Time-Dependent Schrodinger equation for the system.

$$i\hbar\frac{\partial\,\mathbf{\Psi}}{\partial t} = \mathbf{H}\,\mathbf{\Psi} \tag{2.1}$$

This equation can be integrated one step forward in time from time t_0 to time t.

$$\mathbf{\Psi}(t) = \mathbf{\Psi}(t_0) + \frac{1}{i\hbar}\int_{t_0}^{t}\mathbf{H}(t')\,\mathbf{\Psi}(t')\,dt' \tag{2.2}$$

Tully solves for the interaction Hamiltonian, and essentially uses Eq. (2.2) to propagate the wave function. In propagating to the next step he keeps the wavefunction and interaction Hamiltonian constant. Computationally this becomes

$$\mathbf{\Psi}(t) = \mathbf{\Psi}(t_0) + \frac{(t-t_0)}{i\hbar}\,\mathbf{H}(t_0)\,\mathbf{\Psi}(t_0). \tag{2.3}$$

This method is accurate so long as $\mathbf{\Psi}(t')$ and $\mathbf{H}(t')$ are relatively constant during the time step. However, this requires the time step to be very small because of the rapidly spinning electronic phase factors of the different electronic states. The electronic phases are spinning rapidly because of the separation of the different electronic-state

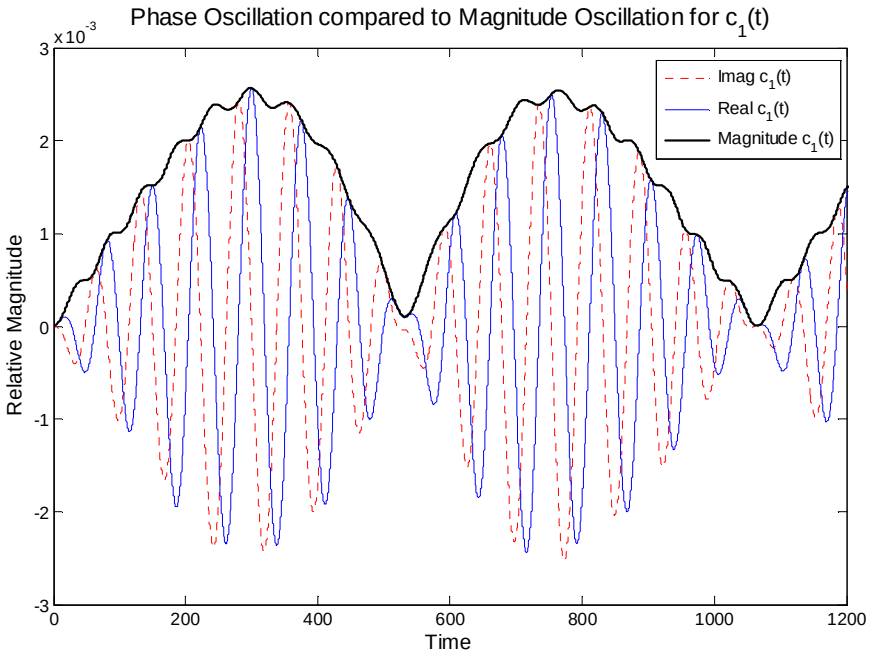

Figure 2.1 Expansion coefficients of the ground state over time in a hypothetical model used to compare the two methods in chapter 3. The real and imaginary phase factors change much more rapidly than the magnitude of $c_1(t)$. The magnitude of $c_1(t)$ does have bumpy features that are close to the phase time scale, but the overall behavior can be categorized on a much larger time scale.

energies. This makes the phase factors the primary limiting factor of the algorithm. Fig. 2.1 shows the difference in time scale of the oscillations of the phase factors and the oscillations of the magnitude of the expansion coefficients. This figure represents the evolution of the ground state coefficients in a hypothetical model used to compare the accelerated and Tully method in chapter 3.

We intend to first improve on the method by using the interaction picture representation to keep track of the phase information. This allows us to integrate over a nuclear motion time scale instead of the electronic time scale. We also use a second-order taylor series expansion in the Hamiltonian for the time step to improve over the approximation of a constant Hamiltonian.

2.2 Interaction Picture Representation

We first separate the electronic Hamiltonian into its time dependent and time-independent parts.

$$\mathbf{H} = \mathbf{H_0} + \mathbf{V}(t) \tag{2.4}$$

The $\mathbf{H_0}$ matrix is a diagonal matrix with the diagonal entries being the energies of the corresponding electronic states. $\mathbf{V}(t)$ contains all of the coupling and time dependence of diagonal elements.

We would like to use the interaction picture representation where the wave function is transformed.

$$\mathbf{\Psi}_I = exp\left(\frac{i\mathbf{H_0}(t-t_0)}{\hbar}\right)\mathbf{\Psi} \tag{2.5}$$

with $\mathbf{\Psi}_I(t_0) = \mathbf{\Psi}(t_0)$.

Schrodinger's equation in the interaction picture becomes

$$i\hbar\frac{\partial\,\mathbf{\Psi}_I}{\partial t} = \mathbf{V}_I(t)\;\mathbf{\Psi}_I \tag{2.6}$$

where

$$\mathbf{V}_I \equiv exp\left(\frac{i\mathbf{H_0}(t-t_0)}{\hbar}\right)\mathbf{V}(t)\;exp\left(\frac{-i\mathbf{H_0}(t-t_0)}{\hbar}\right) \tag{2.7}$$

or more conveniently

$$\mathbf{V}_I \equiv \mathbf{P}^*\,\mathbf{V}(t)\,\mathbf{P} \tag{2.8}$$

where $\mathbf{P}$ is a diagonal matrix made of phase factors $P_{jj} = e^{-i\omega_j(t-t_0)}$ and $\omega_j = \frac{E_j}{\hbar}$. Using the interaction picture, the eigenstates no longer have a spinning phase factor $exp\left(\frac{i\omega t}{\hbar}\right)$, but change only as induced by the interaction potential $\mathbf{V}_I$.

Again the wavefunction can be represented as a superposition of eigenstates, $\phi(\mathbf{r},\mathbf{R})$ with expansion coefficients $c(t)$.

$$\mathbf{\Psi}(t) = \sum_n c_n(t)\,\phi(\mathbf{r},\mathbf{R}) \tag{2.9}$$

Again, $\mathbf{R}$ represents the nuclear positions and $\mathbf{r}$ represents the electronic positions. These eigenstates are eigenfunctions of $\mathbf{H_0}$ without electronic state coupling. They only depend on time through the time dependence of $\mathbf{R}$. Now to put Schrodinger's Equation in matrix form for the interaction picture representation.

$$\begin{aligned} i\hbar\frac{\partial c_k}{\partial t} &= \sum_l \left(\mathbf{P}^*\mathbf{V}\mathbf{P}\right)_{kl}\ c_l \\ &= \sum_l e^{i(\omega_k-\omega_l)(t-t_0)}\ V_{kl}\ c_l \end{aligned} \tag{2.10}$$

2.3 2nd Order Hamiltonian Approximation

The next improvement that can be made to Tully's method is making a better approximation for the Hamiltonian. In Tully's method, this wasn't as necessary due to the small time step required to keep track of the electronic phase information. In our method the error in assuming a constant Hamiltonian for the time step can be more significant due to a larger time step.

We approximate the Hamiltonian using a second-order taylor series centered around the time t_0.

$$\mathbf{H}(t) \approx \mathbf{H}(t_0) + (t-t_0)\,\dot{\mathbf{H}}(t_0) + (t-t_0)^2\,\ddot{\mathbf{H}}(t_0) \tag{2.11}$$

However all of the time dependence in the original Hamiltonian is in the $\mathbf{V}(t)$ term. Therefore,

$$\mathbf{V}(t) = \tilde{\mathbf{H}}(t_0) + (t-t_0)\ \dot{\mathbf{H}}(t_0) + \frac{1}{2}(t-t_0)^2\ \ddot{\mathbf{H}}(t_0) \tag{2.12}$$

where $\tilde{\mathbf{H}}(t)$ is any off diagonal terms in the Hamiltonian and is the interaction Hamiltonian.

$$\tilde{\mathbf{H}}(t) = -i\hbar\ \dot{\mathbf{R}}\cdot\mathbf{d} \tag{2.13}$$

The two derivatives of $\mathbf{H}$ can be found using simple centered finite differences.

$$\dot{\mathbf{H}} = \frac{\mathbf{H}(t+\Delta t) - \mathbf{H}(t-\Delta t)}{2\Delta t} \tag{2.14}$$

$$\ddot{\mathbf{H}} = \frac{\mathbf{H}(t+\Delta t) - 2\mathbf{H}(t) + \mathbf{H}(t-\Delta t)}{(\Delta t)^2} \tag{2.15}$$

2.4 First Order Symbolic Solution

We will now use time-dependent perturbation theory to find a symbolic first order solution to propagate the wavefunction one time step forward, from t_0 to t. In the zeroth order approximation the expansion coefficients are constant in time because the eigenstates don't spin in phase. According to time-dependent perturbation theory [4], and Eq. (2.10) the first order solution is

$$i\hbar \frac{\partial c_k^{(1)}(t)}{\partial t} = \sum_l e^{i(\omega_k - \omega_l)\Delta t}\, V_{kl}\, c_l^{(0)}. \tag{2.16}$$

The zeroth order terms, $c_l^{(0)}$, are constant in time because of the interaction picture representation. In the algorithm they assume the value of the expansion coefficients at the beginning of the time step.

We now integrate this expression to find $c_k^{(1)}(t)$.

$$c_k^{(1)}(t) = c_k(t_0) + \frac{1}{i\hbar}\int_{t_0}^{t} \sum_l e^{i(\omega_k - \omega_l)(t-t_0)} \left(\tilde{\mathbf{H}}(t_0) + (t-t_0)\dot{\mathbf{H}} + \frac{1}{2}(t-t_0)\ddot{\mathbf{H}} \right) c_l(t_0) \tag{2.17}$$

where we have used Eq. (2.11) to replace $\mathbf{V}(t)$.

This integral can be evaluated symbolically using the following integrals.

$$\int t e^{at}\, dt = \frac{(at-1)\, e^{at}}{a^2} + C \tag{2.18}$$

$$\int t^2 e^{at}\, dt = \frac{(2 - 2at + t^2a^2)\, e^{at}}{a^3} + C \tag{2.19}$$

The symbolic solution to Eq. (2.17) is

$$c_k^{(1)}(t) = c(t_0) + \frac{1}{i\hbar}\sum_l \{\ \tilde{H}_{kl}(t_0)\frac{e^{i(\omega_k-\omega_l)(t-t_0)}-1}{i(\omega_k-\omega_l)} \tag{2.20}$$
$$+ \dot{H}_{kl}(t_0)\frac{[i(\omega_k-\omega_l)(t-t_0)-1]\ e^{i(\omega_k-\omega_l)(t-t_0)}+1}{-(\omega_k-\omega_l)^2}$$
$$+ \frac{1}{2}\ddot{H}_{kl}(t_0)\frac{[2-2i(\omega_k-\omega_l)(t-t_0)-(\omega_k-\omega_l)^2(t-t_0)^2]\ e^{i(\omega_k-\omega_l)(t-t_0)}-2}{-i(\omega_k-\omega_l)^3}\}\ c_l(t_0)$$

This is the equation we use instead of Eq. (2.2). Note that the wavefunction is in the interaction representation. After the wavefunction is propagated, it must be transformed back to the Schrodinger representation. In summary to propagate the wave function we use

$$\mathbf{\Psi}_I(t) = (\mathbf{1}+\mathbf{Z})\ \mathbf{\Psi}(t_0) \tag{2.21}$$

where

$$\mathbf{Z}_{kl} = \frac{1}{i\hbar}\ \{\ \tilde{H}_{kl}(t_0)\frac{e^{i(\omega_k-\omega_l)(t-t_0)}-1}{i(\omega_k-\omega_l)} \tag{2.22}$$
$$+ \dot{H}_{kl}(t_0)\frac{[i(\omega_k-\omega_l)(t-t_0)-1]\ e^{i(\omega_k-\omega_l)(t-t_0)}+1}{-(\omega_k-\omega_l)^2}$$
$$+ \frac{1}{2}\ddot{H}_{kl}(t_0)\frac{[2-2i(\omega_k-\omega_l)(t-t_0)-(\omega_k-\omega_l)^2(t-t_0)^2]\ e^{i(\omega_k-\omega_l)(t-t_0)}-2}{-i(\omega_k-\omega_l)^3}\}$$

In using the above equation, if $[(\omega_k-\omega_k)(t-t_0)]$ is very small, roundoff error can be very significant. In that case the following limit can be used for $\mathbf{Z}_{kl}$.

$$\mathbf{Z}_{kl} = \frac{1}{i\hbar}\ \{\ \tilde{H}_{kl}(t_0)(t-t_0) + \frac{1}{2}\dot{H}_{kl}(t_0)(t-t_0)^2 + \frac{1}{6}\ddot{H}_{kl}(t_0)(t-t_0)^3 \tag{2.23}$$

because $e^{i(\omega_k-\omega_l)(t-t_0)} \longrightarrow 1$ in the integral in Eq. (2.17). To increase the stability of the algorithm we use a Crank-Nicolson [5] motivated approach instead of using Eq. (2.21).

$$\mathbf{\Psi}_I(t) = (\mathbf{1}-\mathbf{Z}/2)^{-1}\ (\mathbf{1}+\mathbf{Z}/2)\mathbf{\Psi}(t_0) \tag{2.24}$$

This allows the algorithm to unconditionally stable. Finding a matrix inverse can be computationally intensive, so we rearrange Eq. (2.21) to become solving a linear

matrix problem of the form $\mathbf{A}\ \mathbf{x} = \mathbf{b}$.

$$(\mathbf{1} - \mathbf{Z}/2)\mathbf{\Psi}_I(t) = (\mathbf{1} + \mathbf{Z}/2)\mathbf{\Psi}(t_0) \tag{2.25}$$

and solve for $\mathbf{\Psi}_I(t)$. After solving for $\mathbf{\Psi}_I(t)$, we find $\mathbf{\Psi}(t)$ simply by transforming back to the Schrodinger representation using the $\mathbf{P}$ operator.

$$\mathbf{\Psi}(t) = \mathbf{P}\ \mathbf{\Psi}_I(t) \tag{2.26}$$

In conclusion we found a symbolic first order solution that can be used instead of Eq. (2.2). This allows integrating over the nuclear time scale instead of the electronic time scale. We propagate the wave function ,$\mathbf{\Psi}_I(t)$, by solving Eq. (2.25) with $\mathbf{Z}_{kl}$ determined by Eqs. (2.22), or (2.23). Then we transform $\mathbf{\Psi}_I(t)$ back to $\mathbf{\Psi}(t)$ using $\mathbf{P}$. The rest of the method is the same as Tully's method. In the next section we compare our method with Tully's method to see the difference in computation time and accuracy.

Chapter 3

Results and Conclusions

3.1 Test Model

We used a simple four-state one-dimensional model to compare the accelerated method we have generated with Tully's method. All units are set in atomic units where the mass of an electron, planck's constant, and the speed of light are set equal to one. In these units, the mass of nuclei are set equal to mass of 22000 which is approximately the reduced mass of carbon. The model uses center of mass coordinates with the one dimension representing distance between two nuclei in a diatomic bond. The model is one-dimensional so that $\mathbf{R}$ is equivalent to x. The potentials and coupling were determined by the following interactions in the diabatic representation.

$$\mathbf{H}(x) = \begin{bmatrix} \frac{-\Delta E}{2} & V_1(x) & V_2(x) & 0 \\ V_1(x) & \frac{\Delta E}{2} & 0 & V_2(x) \\ V_2(x) & 0 & \frac{-\Delta E}{4} & V_1(x) \\ 0 & V_2(x) & V_1(x) & \frac{\Delta E}{4} \end{bmatrix} \tag{3.1}$$

where

$$V_1(x) = 6V_0 e^{-A|x|} \tag{3.2}$$
$$V_2(x) = -4V_0 e^{-A|x|}$$

with $V_0 = .8$, $A = 2$, and $\Delta E = 2.4$. The energies, V_0 and ΔE, are then divided by 27.2 to convert them into Hartrees.

Diagonalizing this matrix produces a set of diagonal energies, $D_j(x)$. The eigenfunctions corresponding to this diagonalization can be used to find the nonadiabatic coupling vector using Eq. (1.2). The adiabatic potentials, $E_{0j}(x)$, are acquired by adding two additional potential energy terms representing two hard-wall potentials at $x = 0$, and $x = 2.1$ which represent the presence of other atoms in a solid.

$$E_{0j}(x) = D_j(x) + k\,x^{-4} + k\,(x - 2.1)^{-4} \tag{3.3}$$

where $k = .16$.

These four adiabatic potentials can be seen in Fig. 3.1. As shown in the figure, the initial conditions start with the nuclei being close to equilibrium ($x = 0.9$) in the ground state. The electron is then photo-excited to the fourth state. The nuclei cycles back and forth along the fourth energy surface until the electron eventually falls back down to another state. We ran the simulation using a matrix-solver application software called Matlab. We ran the simulation for 2000 atomic units of time which translate to almost 2 cycles of nuclear motion.

3.2 Method of Comparison and Results

The two methods were coded the same except for the difference in propagating the expansion coefficients, $c_j(t)$. To compare the two methods, we compared the expan-

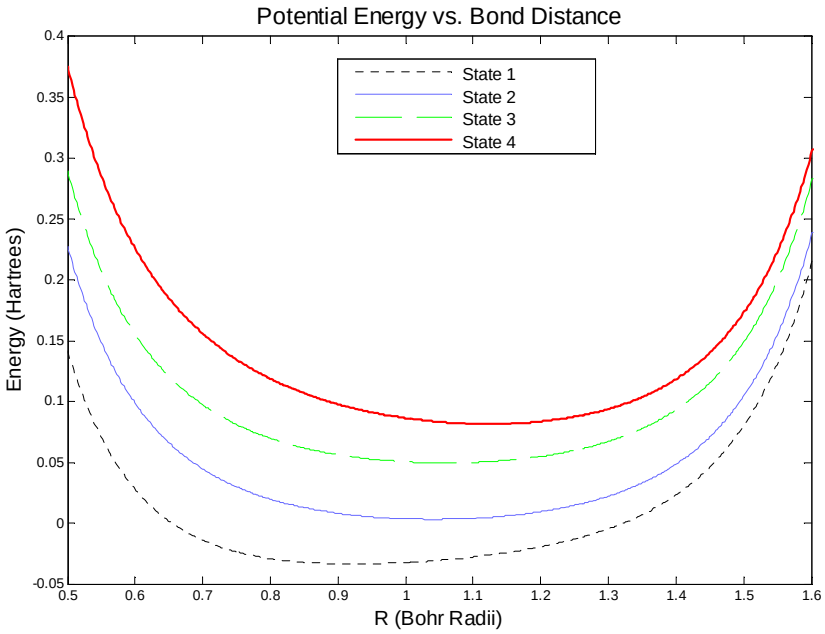

Figure 3.1 Potential energy curves of the hypothetical one-dimensional model we used to compare Tully's method with our accelerated method. The initial conditions are of electron being photo-excited to the fourth state. The nuclei moves along the fourth state surface and eventually the electron falls back down to a lower electronic state.

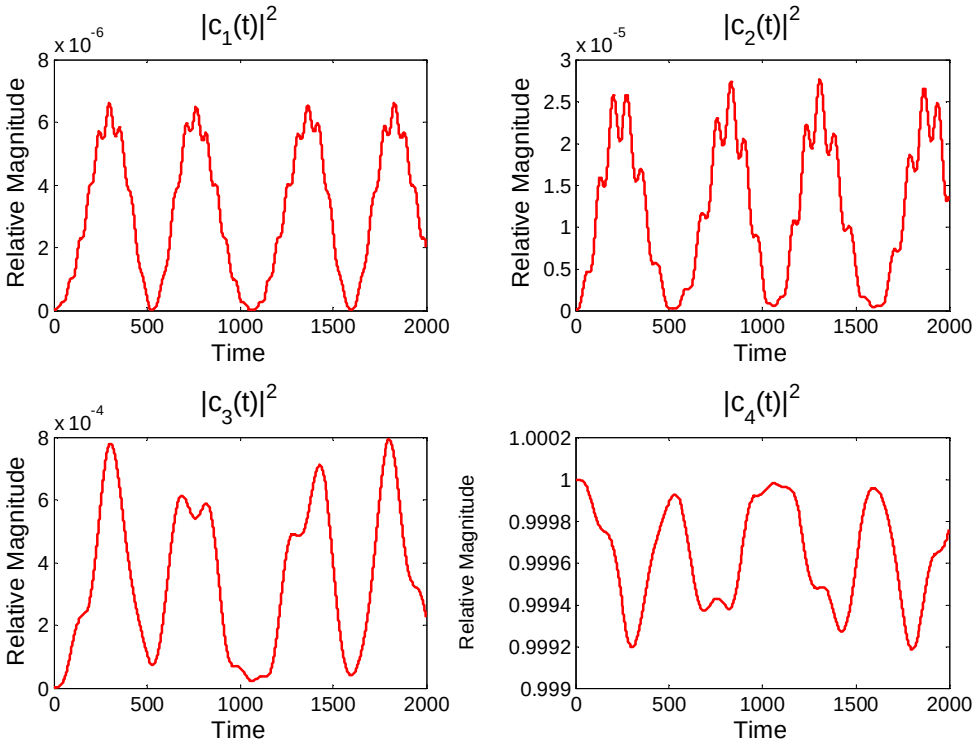

Figure 3.2 Expansion coefficients of the four states for the control group simulation. The model starts with the electron in the fourth state. The third state is coupled the most strongly to state four, and so a transition will most likely occur to the third state.

sion coefficients and switching probabilities over time with varying sizes of time steps used. With a large time step, both methods run the simulation faster, but both are also less accurate. For correct comparison, a control group for the simulation was run with a time step size of .01 atomic units. Both the accelerated method and Tully method converged very closely with this small of time step, so the Tully method was used for the control group.

The expansion coefficients,$|\, c_j(t)|^2$, of the control group simulation are shown in fig. 3.2. The chances of switching to another state in the simulation is very small as can be seen by the small change to the fourth state magnitudes, $|\, c_4(t)|^2$. Because of this, we eliminated any switches to other states. Again, the only difference in our

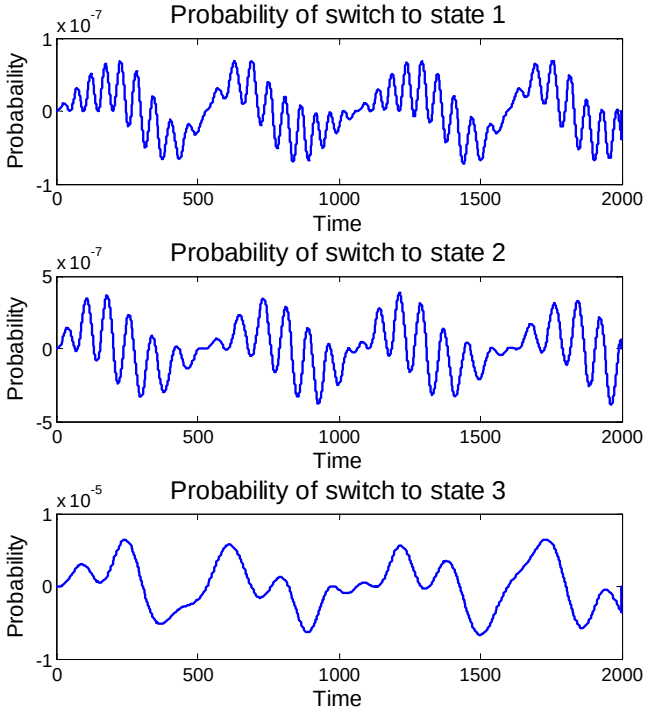

Figure 3.3 The control group switching probabilities during each time step over time. The fourth state isn't calculated because the particle remains in the fourth state.

algorithm is the propagation of the expansion coefficients. The switching probabilities are calculated from the magnitude square of the changing expansion coefficients.

We are most interested in the switching probabilities, because the coefficients are calculated to determine the switching probabilites at each time step. We need to ensure that the switching probabilities remain accurate. Fig. 3.3 shows the control group switching probabilities at each time step. The chance of a switch to state three is much more likely than a switch to the other states.

Because a switch is more likely to occur to the third state, it is this state's expansion coefficients, and switching probabilities that we are most interested in. To compare accuracy we calculated the standard deviation of the third state expansion coefficients curves and switching probabilities curves with the control group curves for different time steps sizes. We divided the standard deviation by the maximum

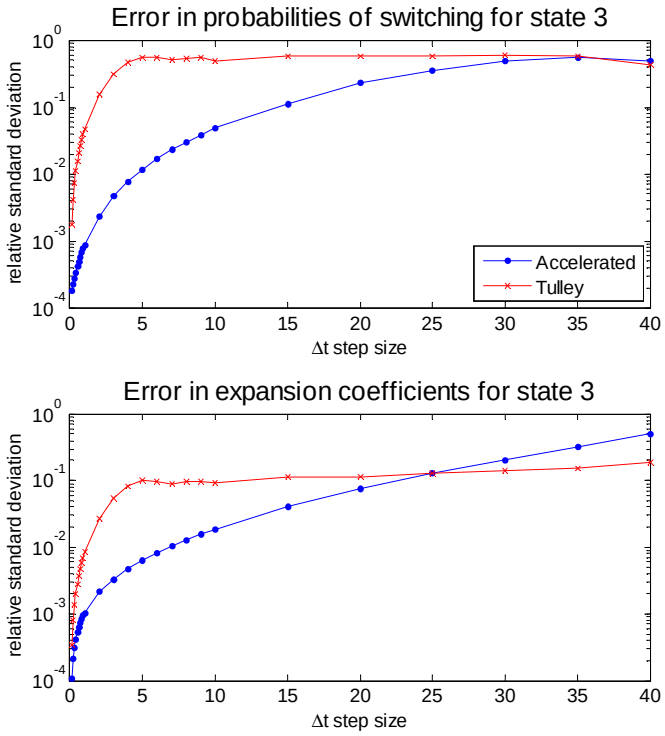

Figure 3.4 Relative standard deviation of the two methods vs. time step size. The error of the accelerated method remains below the error of the Tully method until both methods fail to have any correct significant digits. The Tully method fails this around $\Delta t = 5$, and the accelerated method fails around $\Delta t = 25$.

values of the coefficients and probabilities to get the relative error.

3.3 Results and Conclusions.

Fig. 3.4 shows the relative standard deviation of the two methods for the expansion coefficients and switching probabilities vs. time step size. The error of the accelerated method remains below the error of the Tully method until both methods fail to have any correct significant digits. The Tully method reaches fails around $\Delta t = 5$, and the accelerated method fails around $\Delta t = 25$.

What is most important,however, is the amount of computation time the method

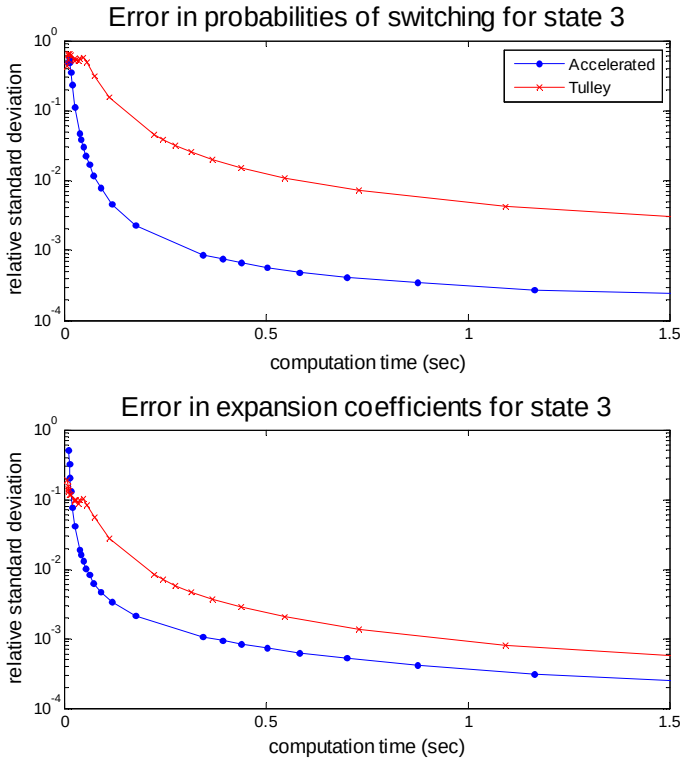

Figure 3.5 Relative standard deviation of the two methods vs. computation time. The accelerated method performs better and is below the Tully method curve except when both methods fail to have any correct significant figures.

takes given a certain level of accuracy. If a method achieves high accuracy but requires too much time to run, the other method can use a smaller time step to achieve the same level of accuracy, and run faster. In our simulations we used a mathematics matrix solving software called Matlab to compare computation times. Fig. 3.5 shows the relative standard deviation vs. computation time for the two methods. The relative standard deviations were calculated the same way as in Fig 3.4.

From the comparison of the error vs computation time, it can be seen that the accelerated method produces more accurate results until both methods fail to have any correct significant digits. In Fig. 3.5, the accelerated method achieves the same level of accuracy in the switching probabilities in about five to ten time less computation time. For example, for an accuracy of two significant digits, the Tulley method takes

about 0.8 seconds, and the accelerated method takes approximately about 0.1 second. The error in expansion coefficients are somewhat closer and the accelerated appears to be two to five times faster. For example, for an accuracy of two significant digits, the Tulley method takes 0.3 seconds, and the accelerated method takes approximately 0.1 second. However, finding the switching probabilities is the goal of calculating the change in expansion coefficients, and so the switching probabilities deviation is the more important comparison.

In the future we would like to incorporate this algorithm into a molecular dynamics package (fireball). It is possible that the results would be improved in a more complicated simulation where the phase oscillation expansion coefficients are even more of a limiting factor due to the number of different states. We also hope to implement a method that changes the step size dynamically to the strength of the interaction of the coupled states. This would allow the method to decrease the step size during strong coupling when a much smaller time scale is needed.

Bibliography

[1] V. May and O. Kuhn, *Charge and Energy Transfer in Molecular Systems*, Wiley, Berlin, 2000.

[2] J. C. Tully, The Journal of Chemical Physics **93**, 1061 (1990).

[3] M. J. Romanelli, *Mathematical Methods for Digital Computers*, Wiley, New York, 1960.

[4] D. J. Griffiths, *Introduction to Quantum Mechanics*, Pearson Prentice Hall, NJ, 2005.

[5] P. Keast and A. R. Mitchell, Computer Journal **9**, 110 (1966).